Athermal martensitic behaviour enhanced in sodium niobate by Mn dopant and axial compression



1997 J. Phys.: Condens. Matter 9 11263

(http://iopscience.iop.org/0953-8984/9/50/026)

J. Phys.: Condens. Matter **9** (1997) 11263–11282. Printed in the UK PII: S0953-8984(97)84998-3

# Athermal martensitic behaviour enhanced in sodium niobate by Mn dopant and axial compression

A Molak

Institute of Physics, University of Silesia, 40-007 Katowice, Poland

Received 6 June 1997, in final form 16 September 1997

**Abstract.** The ferroelastic and antiferroelectric transition (between phases called P and R) in $NaNbO_3$ samples, pure and doped with Mn (0–3.3 mol%), was investigated. The phase diagram was obtained from DTA tests. The doping resulted in lowering of the P–R phase transition temperature. The shift of the P–R phase transition temperature was observed also in dielectric permittivity $\varepsilon(T)$ measured under compression. Changes in enthalpies obtained from DTA were compared to the latent heat values calculated independently from the Clapeyron–Clausius equation. Values of thermodynamic parameters of the P–R phase transition were evaluated. The EPR test showed that the Mn dopant causes disorder and local strains. Athermal martensitic behaviour of the P–R phase transition in $NaNbO_3$ was enhanced by applied compression and the dopant subsystem.

## 1. Introduction

The mechanical and electrical properties near phase transformations in ferroelastic perovskites with ferroelectric or antiferroelectric order have attracted studies during recent years. It has been found that thermodynamic parameters of the perovskites depend strongly on chemical composition, dopant concentration and applied external fields [1, 2]. The martensitic aspects of the ferroelastic transitions in perovskites are recognized less commonly. Generally, two classes of isothermal and athermal martensitic transformations are known. The first proceeds at a constant temperature in some finite time. The second develops, under defects or stress influence, in a temperature interval, while fracture volumes of a parent phase transform into martensite phase [3, 4].

An actual first-order phase transition develops in complicated conditions especially when the martensite phase nucleates around defects. The description of the phase front kinetic is supported on the time-dependent Landau–Ginzburg equation. The kink-type solution represents the interface boundary which velocity is scaled with such factors as defects concentration, solid solution composition, electric field or external stress [5–8].

The unstable movement of the interphase boundary in perovskites, namely a switching between slow and rapid motion of the boundary, is seen by direct optical observation [9, 10]. A hypothesis has been formulated that the jerky motion of the phase front is affected by relaxational processes of mechanical stresses at the phase boundary [11]. Therefore the course of the transition should be governed not only by the symmetry change but also would be influenced by local strains caused by the defects or dopants. Moreover, the kinetics of the phase front can be by affected by temperature variations due to latent heat

0953-8984/97/5011263+20$19.50  

generation near the interphase boundary [10]. However, it has been pointed that high heat conductivity reduces the importance of the latent heat release [7].

A convenient perovskite for such an investigation is sodium niobate of which the structural and electrical properties are very sensitive to various internal and external factors. $NaNbO_3$ exhibits a series of stable phases (cubic, $T_2$, $T_1$, S, R, P, N) and after that metastable phases are recognized also [12–15]. Electric properties of sodium niobate are influenced by hydrostatic pressure [16]. The EPR investigation of $NaNbO_3$ crystals doped with Mn shows distinct and sharp changes of crystal field at the structural phase transitions of the first order [17], in agreement with the x-ray results [12–14]. Finally, the occurring structural transformations are sensitive to defects introduced into the crystal lattice. For instance, the temperatures of these phase transitions are markedly shifted with dopant concentration (K, Li, Ca, Gd, Ta, Sr, Mn) [18–23]. The main anomaly in dielectric permittivity of $NaNbO_3$ is connected to the ferroelastic and antiferroelectric first-order transition between phases called P and R [10, 13, 24]. The influence of defects on dielectric permittivity of $NaNbO_3$:Mn has been found [25, 26] but the thermodynamic parameters of the phase transitions have not been evaluated. There is still an open question if and how a non-stable jerky motion of the phase front is reflected in the classic measurement of dielectric permittivity.

There are two aims of this work. The first is the estimation of the thermodynamic parameters of the antiferroelectric–ferroelastic phase transition in sodium niobate: transition temperature shift under compression $\partial T_{tr}/\partial p$, phase transition dependence on dopant concentration $T_{tr}(n)$, changes in enthalpy $\Delta H$ and entropy $\Delta S$ of the transition. The second is the indirect investigation of this phase transition kinetics.

## 2. Experimental details

Single crystals of pure $NaNbO_3$ were grown by the flux method from melted salts solution [27]. Non-oriented multidomain rectangular bars were chosen for the experiment. Ceramics of sodium niobate doped with manganese were sintered according to the standard procedure. Manganese oxide (Aldrich, purity $\geqslant$ 99%) was added to the stoichiometric mixture of $Na_2CO_3$ (Reachim, purity $\geqslant$ 99.8%) and $Nb_2O_5$ (Fluka, purity $\geqslant$ 99.9%). The mixtures were prepared to obtain $N_{Mn} = 0.0, 0.05, 0.1, 0.1, 0.2, \ldots, 1.0$ wt% of Mn in the ceramic samples—these amounts correspond to a series of samples containing from 0 up to 3.3 mol% of Mn [22]. It should be mentioned that an uncontrolled small amount of impurity ions, originating from initial substrates, may be present even in the nominally pure samples.

The DTA test was performed using Unipan DSC 605 equipment. The crushed ceramics with diameters of $\sim$0.1–1 mm were enclosed in gaskets. The DTA signals were recorded in the 300–700 K range while temperature change rates were 5 or 8 K min$^{-1}$.

The EPR test was performed using an Unipan spectrometer. The spectra were recorded in the X-band at room temperature [22].

The electric permittivity was measured with a Tesla BM 595 capacitance meter within the temperature range 300–750 K at a constant rate of temperature change 1 K min$^{-1}$. The measuring frequency was equal to 20 kHz. The electrodes were painted with Ag or Pt paste and fired. Axial compression was applied to the bar samples with the use of a lever and a weight within the range of 1000 bar. The electrodes were perpendicular to the applied compression. Electric permittivity was recorded under constant pressure in subsequent cycles of heating and cooling.

## 3. Results

### *3.1. DTA test*

The recorded DTA signals show the evolution of a phase transition as a function of Mn dopant concentration. In the nominally pure sodium niobate, an antiferroelectric phase transition between phases called P and R is seen at 633 K on heating. This DTA peak is shifted toward lower temperatures when the Mn content in the samples is increased. This anomaly is diffused for the samples containing more than 1.3 mol% of Mn.

Another broad DTA anomaly may be distinguished in the sodium niobate samples at Mn content equal to 0.66 or 1.0 mol% but its temperature range could not be determined precisely. When the manganese concentration is higher then this anomaly develops into a peak. The induced peak, observed at 660–670 K on heating, is connected to the phase transition between phases I and R (see figure 1(a) and table 1). The changes (induced by Mn dopant) observed on cooling are similar (see figure 1(b)). However, one could notice an additional anomaly appearing (around 575 K) on the cooling run for the nominally pure sample. This could be probably the manifestation of a metastable phase caused by uncontrolled defects. In fact, the undoped ceramic samples contain impurities—it has been stated that EPR spectra originating from the $Mn^{2+}$ ions are detected even for the undoped, nominally pure, ceramic samples of $NaNbO_3$.

The phase diagram (temperature of DTA peak against Mn concentration) obtained from DTA tests is presented in figure 2. The transition between phases P and R is observed in the nominally pure and in the slightly doped ceramics. The sequence of phase transitions—between the phase P (known from pure sodium niobate), the phase I (induced by Mn dopant) and the phase R—occurs at intermediate Mn concentration. The former x-ray investigation showed that the phases P and I may coexist in sodium niobate at these intermediate Mn contents [23]. The phase transition between the R phase and the induced I phase only is observed at Mn concentration high enough ($\geqslant$2 mol%).

### *3.2. Dielectric permittivity*

The measurement of dielectric permittivity $\varepsilon(T)$ performed on $NaNbO_3$ crystals under compression shows two main effects. Firstly, the maximum in electric permittivity is shifted toward lower temperatures. Secondly, the compression results in a change of $\varepsilon(T)$ characteristic shape in the vicinity of the P–R phase transition. The sharp jump in $\varepsilon$ value at the temperature of the phase transition is observed when the sample is not compressed (see figure 3(a)). In contrast, several steps appear on the $\varepsilon(T)$ curve in the range of the investigated phase transition when the applied pressure exceeds a few hundred bars ($\geqslant$150 bar). The changeover from the steplike $\varepsilon(T)$ characteristic to a rounded one is observed when the pressure is increased (see figure 3(b), (c)). The compression causes the crossover from the sharp transition appearing as one jump in a range less than 0.05 K (temperature has been recorded at $\approx$3 s periods) under 1 bar to a wide gradual transformation developing within a few or several K range. Such a behaviour may be explained by jerky motion of phase front. The P–R interphase boundary, driven by temperature change, is expected to move with a certain velocity. On the other hand, the phase front moving through the sample may be blocked many times on local strains or defects. Due to these competing effects, transformation of fractal volumes of the sample results in the mixed state of the phases P and R coexisting in the compressed sample. Their contributions to the

**Table 1.** Data concerning the antiferroelectric and ferroelastic P–R phase transition (obtained on heating) for sodium niobate doped with manganese (0–3 mol%). The left column has been obtained from DTA: transition temperature $T_{DTA}$, enthalpy $Q_{DTA}$ and entropy change $\Delta S_{DTA}$. The right column has been calculated from $\varepsilon(T, p)$ data: transition temperature $T_a$, transition temperature shift under compression $\mathrm{d}T_a/\mathrm{d}p$, latent heat $L$ and corresponding entropy change $\Delta S_L$. $\Delta V$ denote the elementary cell volume known from x-ray data [13]. The $BaTiO_3$ data, taken from the literature [34], are given for comparison.

| | DTA $\Delta S_{DTA} = Q_{DTA}/T_{DTA}$ | | | | $\varepsilon(T, p)$ $L = T_a \Delta V/(\mathrm{d}T_a/\mathrm{d}p)$ $\Delta S_L = L/T_a$ | | | | |
|---|---|---|---|---|---|---|---|---|---|
| Phase transition | $N_{Mn}$ (mol%) | $T_{DTA}$ (K) | $Q_{DTA}$ (J mol$^{-1}$) | $\Delta S_{DTA}$ (J mol$^{-1}$ K$^{-1}$) | $T_a$ (K) | $\mathrm{d}T_a/\mathrm{d}p$ (K kbar$^{-1}$) | $\Delta V$ (cm$^3$ mol$^{-1}$) | $L$ (J mol$^{-1}$) | $\Delta S_L$ (J mol$^{-1}$ K$^{-1}$) |
| P–R | 0 | 633 | 220 | 0.33 | 633 | −5 | −0.027 [13] | 340 | 0.54 |
| P–R | 0.33 | 608 | 230 | 0.36 | | | | | |
| P–R | 0.66 | 611 | 360 | 0.58 | | | | | |
| P–R | 1.3 | 590 | — | — | | | | | |
| I–R | 1.3 | 670 | — | — | | | | | |
| I–R | 2 | 672 | 350 | 0.52 | | | | | |
| I–R | 3 | 663 | 360 | 0.53 | | | | | |
| Crystal $NaNbO_3$ | | | | | | | | | |
| P–R | — | 644 | 210 | 0.32 | 626 | −6 | −0.027 [13] | 280 | 0.45 |
| Crystal $BaTiO_3$ [34] | | | | | | | | | |
| Tet–cub | | 397 | 210 | 0.53 | 397 | −5.8 | −0.022 | 150 | 0.39 |

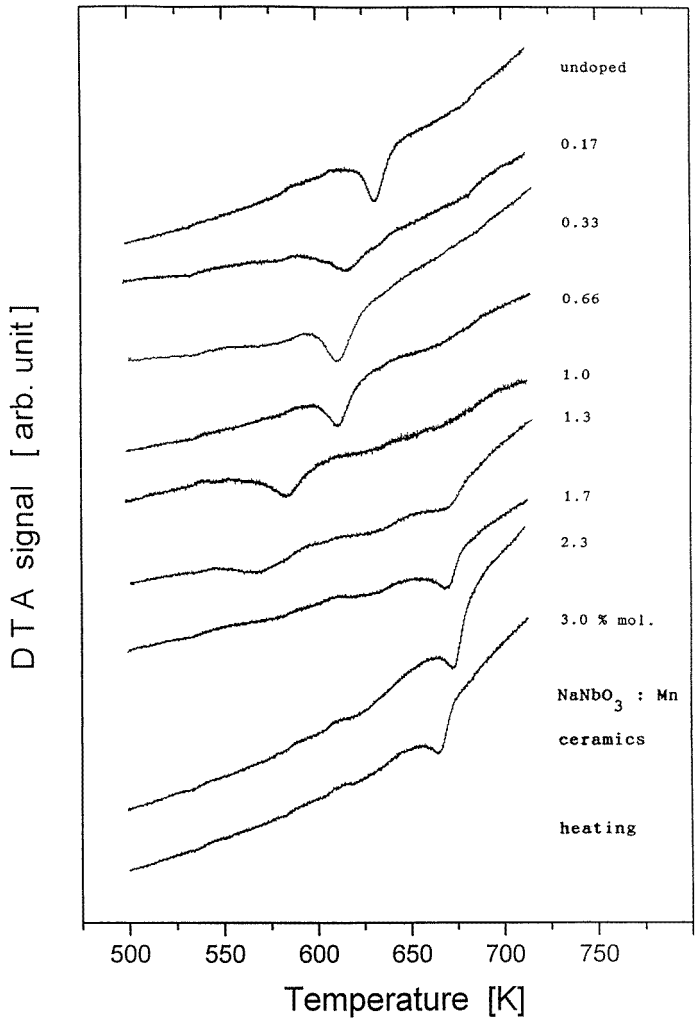


(a)

**Figure 1.** DTA signal against temperature recorded for ceramic samples of $NaNbO_3$ doped with manganese (Mn content varies from 0 to 3 mol%): (a) heating, (b) cooling.

dielectric permittivity lead to the measured value

$$\varepsilon \cong \left(\frac{V_P}{\varepsilon_P} + \frac{V_R}{\varepsilon_R}\right)^{-1} \tag{1}$$

where $V_P$ and $V_R$ are the relative volumes ($V_P + V_R = V_{SAMPLE}$) of the P and R phases with permittivity $\varepsilon_P$ and $\varepsilon_R$, respectively. One can say that successive change of measured value of dielectric permittivity is reflected by the steplike $\varepsilon(T)$ shape connected to a variety of transition temperatures.

Additionally, a statistical spread of $\varepsilon(T, p)$ values is detected above the phase transition, especially for compressed samples. It should be mentioned that the temperature in which the dielectric permittivity reaches its maximal value cannot be regarded as an apparent

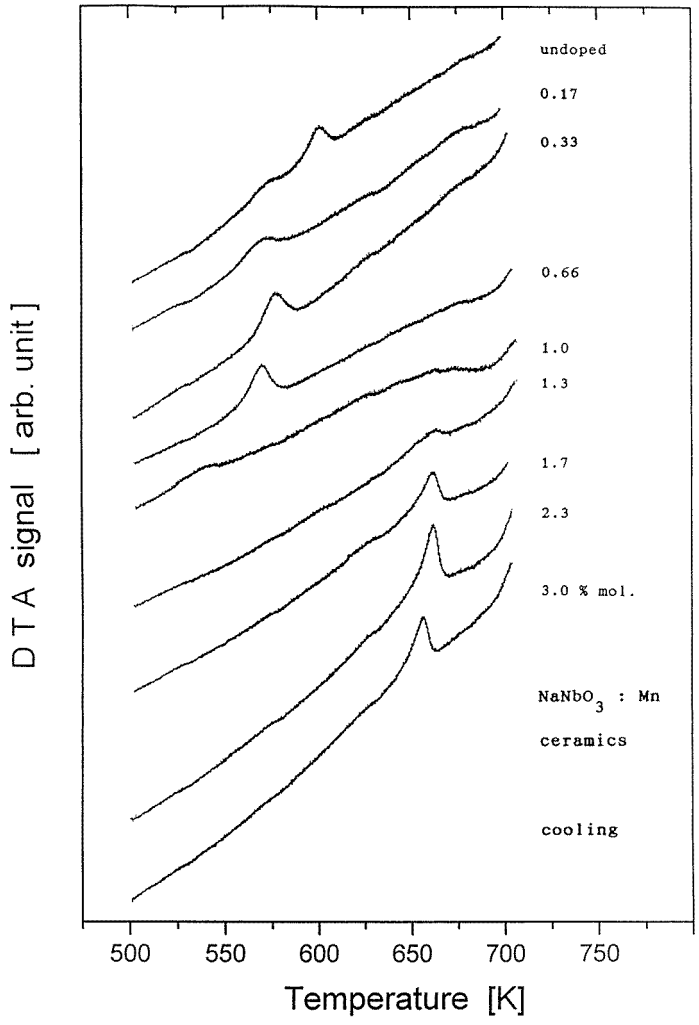


(b)

**Figure 1.** (Continued)

temperature of the phase transition under external pressure. Instead of this, the other way for determination of the mean temperature of the phase transition may be proposed. The main jump in the $\varepsilon(T)$ characteristic is taken for evaluation of the phase transition temperature $T_{P-R}$ shift under pressure. The transformation, or the phase front movement, is most effective at the temperature which corresponds to maximal values in the derivatives of recorded dielectric permittivity $\Delta\varepsilon/\Delta T$. The $(\Delta\varepsilon/\Delta T)$–$T$ dependencies have been calculated for each $\varepsilon(T, p)$ data set. Those obtained at $p = 1, 500$ and 900 bars are inset into figure 3(a)–(c) for evidence. The obtained values of $T_{P-R}$ shifted by the applied pressure lead to $\partial T_{P-R}/\partial p = -6 \pm 1$ K kbar$^{-1}$ on heating and approximately 0 K kbar$^{-1}$ on cooling (see figure 4).

Similar effects are observed in the case of ceramic samples of sodium niobate. The dielectric permittivity dependencies on temperature recorded under compression show

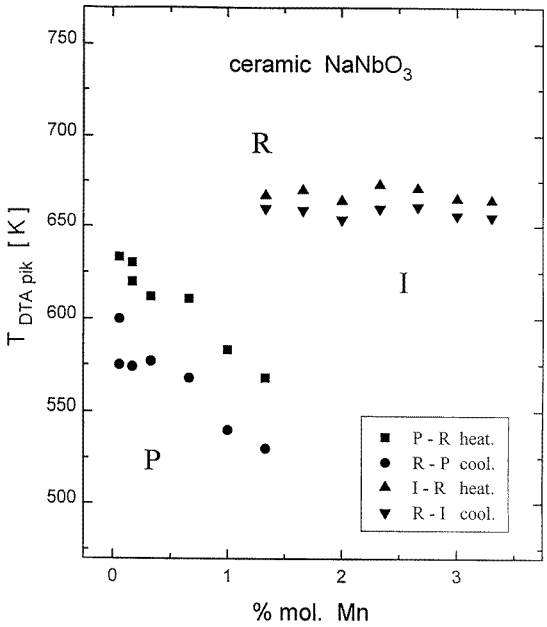


**Figure 2.** Phase diagram of $NaNbO_3$:Mn (temperature against Mn dopant concentration) obtained from DTA data. Transition P–R is known from pure sodium niobate. Transition I–R is induced by the manganese dopant.

rounded maxima around the phase transition temperature (see figure 5). The maximum in the $\varepsilon(T)$ curves is well defined and thus the value $\partial T\varepsilon_{max}/\partial p$ may be interpreted as the temperature shift of the transition between phases P and R. The temperature $T(\varepsilon_{max})$ is lowered on heating with the rate $\partial T_{P-R}/\partial p = -5 \pm 1$ K kbar$^{-1}$. This shift value obtained from cooling processes is $\partial T_{P-R}/\partial p = -1.5 \pm 1$ K kbar$^{-1}$ (see figure 6). This value is close to the value obtained for the P–R phase transition in the undoped sodium niobate crystal. Higher values of the P–R phase transition shift in ceramic sodium niobate are received from the calculated dependency of derivatives $\Delta\varepsilon/\Delta T$ on temperature, namely $\partial T_{P-R}/\partial p = -7 \pm 1$ K kbar$^{-1}$ on heating and $\partial T_{P-R}/\partial p = -5 \pm 1$ K kbar$^{-1}$ on cooling.

### *3.3. EPR test*

The EPR test shows the spectra originating from $Mn^{2+}$ centres (see figure 7). The EPR h.f.s. spectra connected to $Mn^{2+}$ ions are traced even for nominally pure $NaNbO_3$ ceramic [22]. The unavoidable amount of manganese ions appear as an impurity contained in chemicals used for sintering. The determination of this Mn amount (supported on the spectra intensity comparison) gives the approximate concentration 0.01 mol% in the nominally pure ceramic samples. The h.f.s. spectrum of $Mn^{2+}$ ions ($g = 2.00$, $|A| = 78 \times 10^{-4}$ cm$^{-1}$) is recorded only for the slightly doped ceramics when the Mn content is lower than 1 mol%. This spectrum can be ascribed to the isolated paramagnetic centres [17, 28]. If the manganese content in ceramics is higher then a broad resonant line ($\Delta H \cong 0.04$ T) coexists together with the h.f.s. spectrum. This broad resonant line dominates the h.f.s. spectrum when the Mn concentration exceeds 2 mol%. Such an evolution of EPR signal with the manganese content variation indicates the gradual transformation of paramagnetic $Mn^{2+}$ centres.

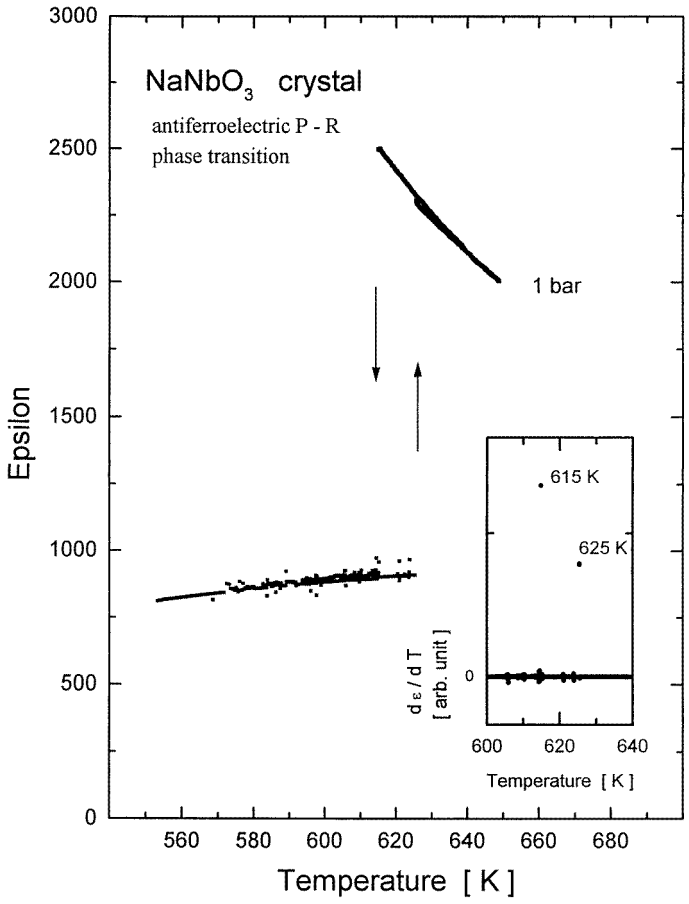


(a)

**Figure 3.** Dielectric permittivity against temperature of the $NaNbO_3$ single crystal, recorded around the ferroelastic and antiferroelectric P–R phase transition. Characteristic shape is (a) one-step jump, sample at atmospheric pressure = 1 bar; (b) several steps in the range of the P–R transition, sample under compression 500 bars; (c) rounded (or many steps) in the range of the P–R transition, sample under compression 900 bars. The insets show the derivative $\Delta\varepsilon/\Delta T$ values calculated around the P–R transition. Their maximal values may be interpreted as occurring at the effective transition temperature. The intervals with high values of $\Delta\varepsilon/\Delta T$ are delimited with starting $T_S$ and martensite $T_M$ temperatures connected to the martensitic athermal transformation.

These recorded EPR spectra of paramagnetic centres reflect the crystal field of the lattice around the dopant ions. Thus, they should bring information about the existing local symmetry and its deformation. Such an effect has been discussed in a paper concerning Mn spectra in disordered materials [29]. In polycrystalline and disordered materials, the outer fine-structure transitions (other than the central hyperfine sextet) in the $Mn^{2+}$ EPR spectrum broaden out due to random orientations of the paramagnetic centres. The forbidden hyperfine lines belonging to the hyperfine central sextet may be broadened out also in single-crystal and polycrystalline materials, in such a case due to strain effects, random orientations of $Mn^{2+}$ ions or dipolar orientations. One can deduce that the visible crossover in the EPR

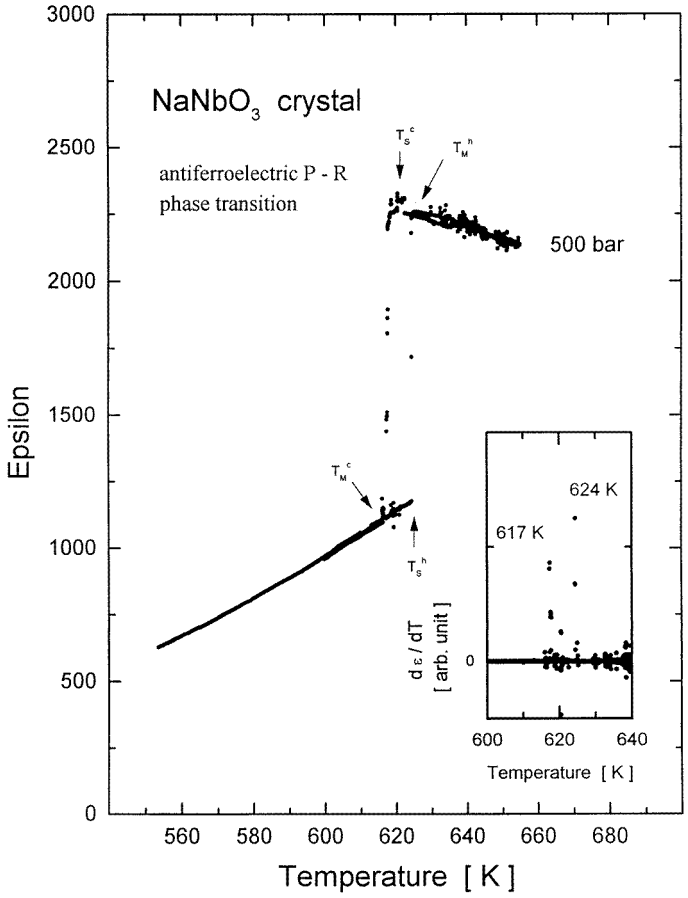


(b)

**Figure 3.** (Continued)

spectra recorded for the samples of $NaNbO_3$:Mn indicates the growing disorder and/or strains when the Mn content is increased.

## 4. Calculations and discussion

It has been shown within the Landau theory that the uniaxial pressure conjugated to strain shifts the temperature of the first-order phase transition [1, 2, 4]. After that the kinetic properties of structural phase transitions in perovskites are affected by defects and dopants [1, 7, 30, 31]. Thus, such effects have to be expected in ferroelastic and antiferroelectric transition in sodium niobate. The investigation of the P–R phase transition occurring in pure and Mn doped sodium niobate shows that this phase transition is affected both by external compression and by internal fields caused by doping.

The defect subsystem role has been widely investigated and discussed in the literature. The isolated defect regime of low concentrations includes both slight doping with ions purposely introduced into the samples and also unavoidable defects originating from the technology process. The increase in doping concentration leads through ‘quasi-isolated’

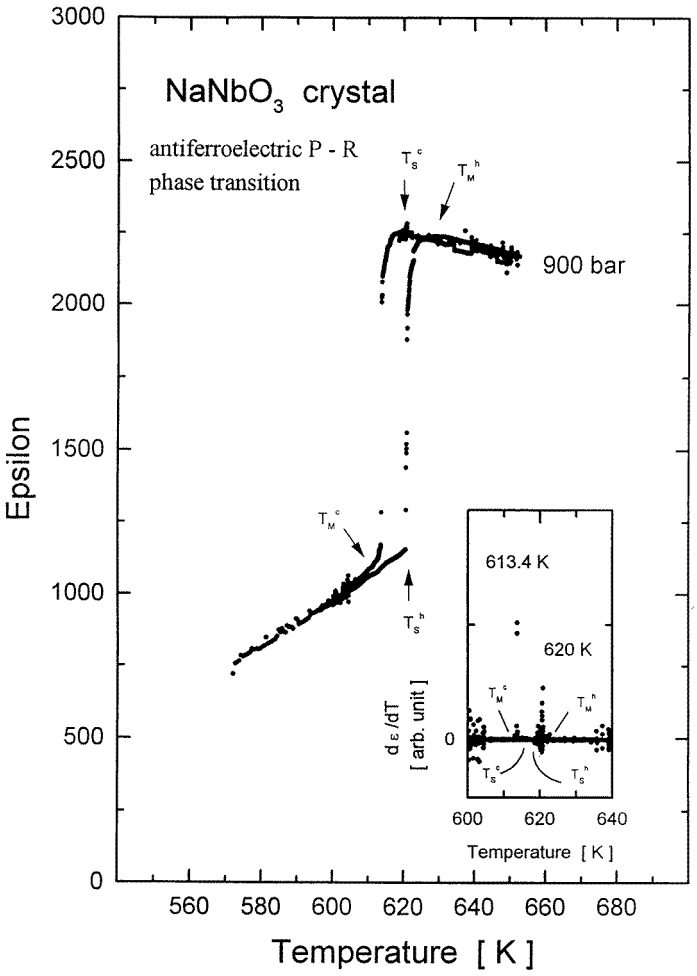


(c)

**Figure 3.** (Continued)

defects to interacting defects. The change of phase transition temperature is then a linear function of the defect density. At defect (or dopant) concentrations $N_{def}$ high enough, usually a few molecular %, homogeneous fields develop and linear change in phase transition temperature is expected [1, 32, 33].

A linear change of the P–R phase transition temperature $T_{P-R}$ is observed in sodium niobate ceramics with Mn dopant concentration $N_{Mn}$ increasing from 0.3 to 1.3 mol%. On the other hand the crystal field disorder in the $NaNbO_3$:Mn samples has been deduced from the EPR spectrum evolution. Therefore, one may classify the manganese dopant (within the concerned concentration range) in sodium niobate as a subsystem of quasi-isolated or interacting defects.

The Mn dopant subsystem introduces a marked contribution to the enthalpy change in the investigated P–R phase transition. The transition enthalpy values (based on DTA) were obtained as averages from several records and they were estimated with an accuracy of

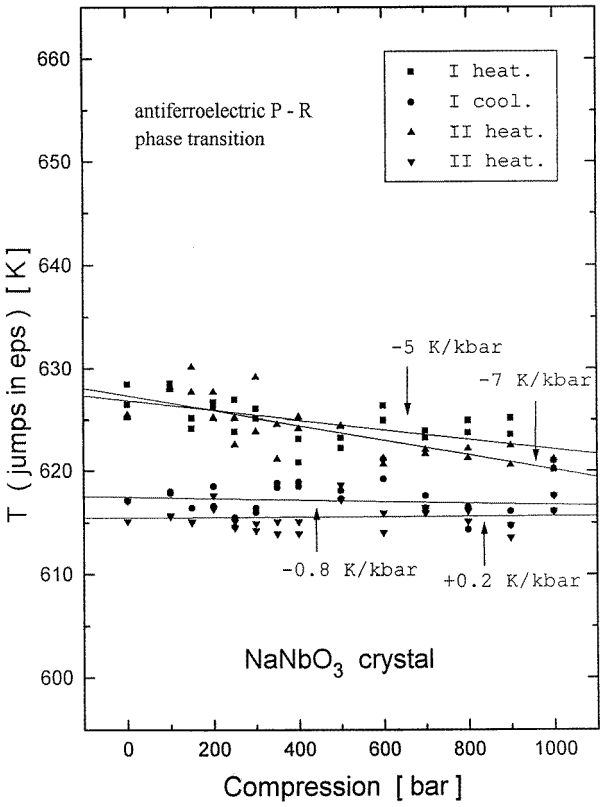


**Figure 4.** Ferroelastic and antiferroelectric P–R phase transition temperature against axial compression received from maxima in derivatives $\Delta\varepsilon/\Delta T$ of dielectric permittivity $\varepsilon(T, p)$ characteristics of $NaNbO_3$ crystal. Linear fits are shown: $-5$ K kbar$^{-1}$ (first heating), $-7$ K kbar$^{-1}$ (second heating), $-0.8$ K kbar$^{-1}$ (first cooling), $+0.2$ K kbar$^{-1}$ (second cooling).

about 20%. These $Q_{DTA}$ values increase from 220 J mol$^{-1}$ up to 360 J mol$^{-1}$ with the Mn dopant concentration change (see table 1).

The experimental value of transition heat measured by the DTA method includes such terms as latent heat of transition $\Delta H_{tr} = L$, elastic enthalpy $\Delta H_{elast}$, enthalpy of defects subsystem $\Delta H_{def}$ and enthalpy due to change in electric order $\Delta H_{el.ord}$. Several other contributions from space charge, domain walls etc are usually comparatively small and thus can be omitted [34, 35]. One can write the change in measured enthalpy

$$\Delta H = \sum_i \Delta H_i = \Delta H_{tr} + \Delta H_{elast} + \Delta H_{def} + \Delta H_{el.ord} + \cdots. \tag{2a}$$

The overall entropy change includes the corresponding terms

$$\Delta S = \Delta S_L + \Delta S_{elast} + \Delta S_{def} + \Delta S_{el.ord} + \cdots. \tag{2b}$$

The Clapeyron–Clausius equation allows us to calculate the latent heat $L$ of the transition since the temperature of the transition $T_{tr}$ and its shift under compression are known from the dielectric permittivity measurement, the change in elementary cell volume $\Delta V$ is known from x-ray data [13]

$$\Delta H_{tr} = L = T_{tr}\,\Delta V/(\partial T_{tr}/\partial p) \tag{3a}$$

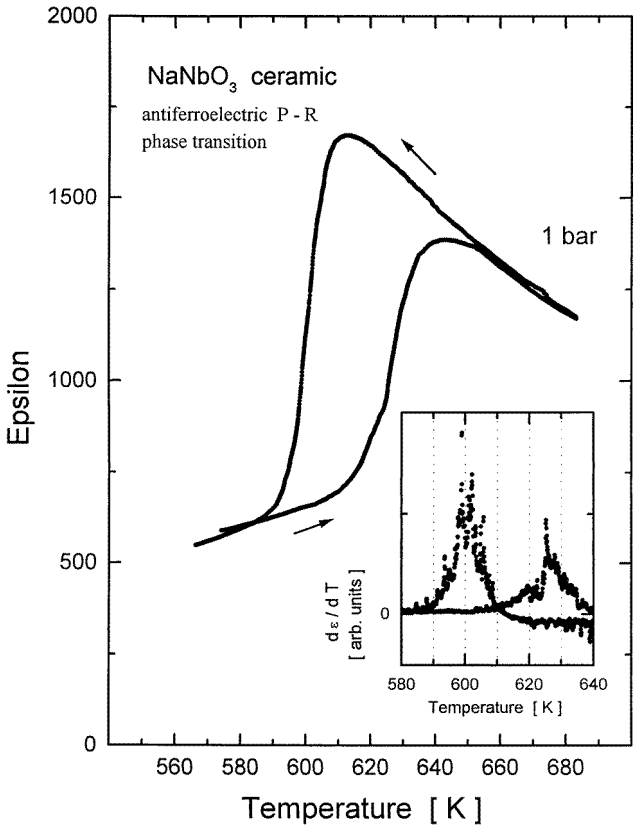


(a)

**Figure 5.** Dielectric permittivity against temperature of the undoped $NaNbO_3$ ceramic recorded at atmospheric pressure (1 bar) and under axial compression (500 and 900 bars). The insets show the derivative $\Delta\varepsilon/\Delta T$ values calculated around the P–R transition. Their maximal values may be interpreted as occurring at the effective transition temperature.

and the co-change in entropy equals

$$\Delta S_L = L/T_{tr}. \tag{3b}$$

The calculated values of $L$ and $\Delta S_L$ received from measured $\varepsilon(T, p)$ dependencies (see figures 4 and 6) are shown in table 1.

The elastic component of the enthalpy change $\Delta H_{elast}$ connected to the transformation interacting with the stresses may be resolved into two terms: (i) a shear stress $X_s$ times amount of the shear strain $e_s$ and (ii) a normal stress $X_n$ times a linear component $e_n$ of the volume change accompanying the transformation [34, 36] and thus

$$\Delta H_{elast} = \sum X_s e_s + \sum X_n e_n. \tag{4}$$

The enthalpy of the defect subsystem $\Delta H_{def}$ reflects the interaction between the phase front moving during the transition and crystal lattice defects. The concerned sodium niobate samples contain usually such point defects as oxygen vacancies [26]. The doping with Mn ions creates additional point defects and even volume defects like precipitation [25]. These defects can act as stress concentrators which form dislocations in their vicinity

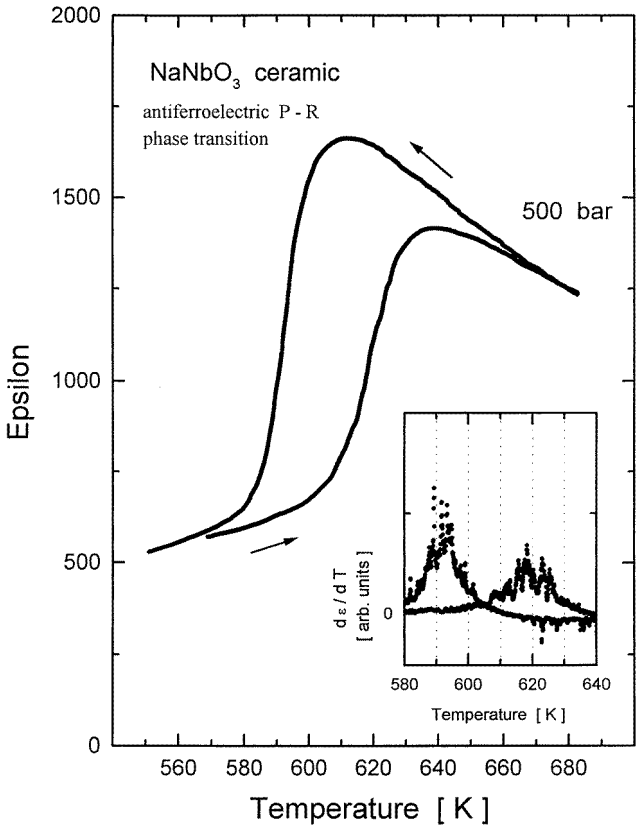


(b)

**Figure 5.** (Continued)

[37]. The increase in dislocation density, caused by doping or external load, leads to the mutual interaction between dislocations. The stored energy can be released if the dislocations rearrange into other configurations like the boundaries. Another important origin of dislocation boundaries is interfaces between the parts of the crystal with different symmetry. A matching of the interface between two phases with different atomic spacing $a_1$ and $a_2$ can be achieved if the misfit parameter $(a_2 - a_1)/a_1$ is small. In this case, the elastic coherency strains can be accommodated by the formation of an array of edge dislocations at the interface boundary. The stress field, strain energy, movement and other properties of such a boundary will depend on the type of dislocation present in the boundary. On the other hand, the interface movement is influenced by temperature, external stress and the capture phenomena on obstacles. The variety of imperfections encompasses the range from small barriers such point defects (from vacancies or solute dopant ions) up to large barriers such as precipitates. The obstacles produce short-range barriers which can be overcome by thermal activation and/or the flow stress. Overcoming the barrier requires changes in energy provided in the form of mechanical work done by the applied load and the thermal activation [37–40]. Hence, these processes form the defect part of the enthalpy change during the phase transition.

The analysis (presented in this paper) of equation (2) follows in analogy to the literature example [34] of transition between tetragonal ferroelectric and cubic paraelectric

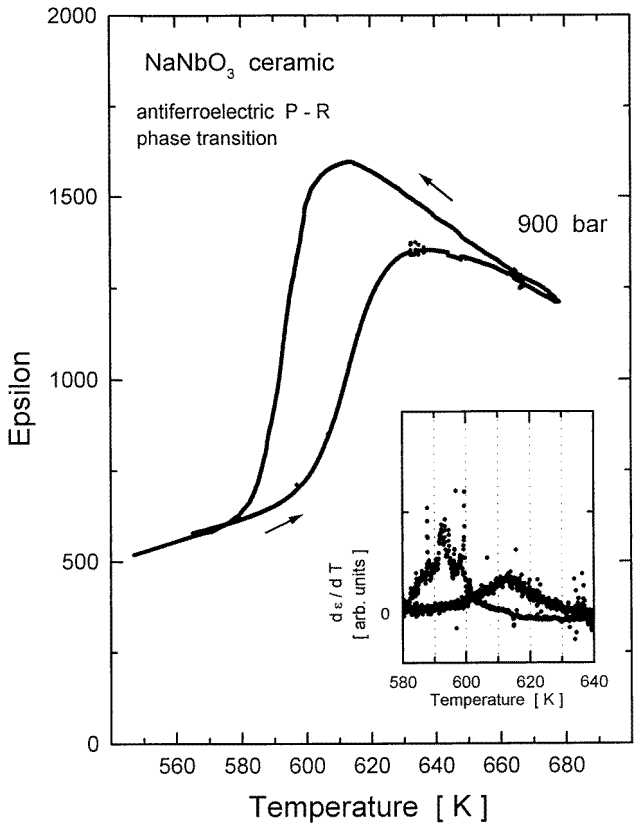


(c)

**Figure 5.** (Continued)

phases in $BaTiO_3$ where latent heat $L = 150$ J mol$^{-1}$, whereas polarization gives $\Delta H_{el.ord} = \Delta H_{FE-PE} = (\beta/2\varepsilon_0)P_s^2 = 253$ J mol$^{-1}$. Necessary approximations for relations between the shear and normal stresses and strains (such as $X_s = X_n$, $X_n = c_{44}e_{23}$, $c_{44} = 5.43 \times 10^{-10}$ N m$^{-2}$, $e_{23} \approx \varphi' \cong 0.0058$, $\varphi'$ denotes angular deformation) are made and numerical values of stiffness constants $c_{ij}$ are used to obtain $\Delta H_{elast} = \alpha(c_{44}\varphi')^2$ J m$^{-3}$ (where calculated coefficient $\alpha \cong 0.5 \times 10^{-10}$ m$^2$ N$^{-1}$). The conducted calculation leads therefore to the value $\Delta H_{elast} = -195$ J mol$^{-1}$. Consequently, the effective sum

$$\sum_i \Delta H_i(BaTiO_3) = 150 + 253 - 195 = 207 \text{ J mol}^{-1} \tag{5}$$

remains in good agreement to the value obtained from DTA as $Q_{DTA} = 205$ J mol$^{-1}$ [34] (placed in table 1 for comparison).

The difference between the $Q_{DTA}$ results measured for $NaNbO_3$ samples and the latent heat $L$ calculated (3*a*) from dielectric permittivity $\varepsilon(T, p)$ data increases when the Mn concentration is higher. Thus, one may state that the latent heat contributes as a part only of the effective transition heat value $\Delta H$ (2*a*) measured by DTA. The amount lacking in enthalpy could be related mainly to elastic effects, denoted as $\Delta H_{elast}$, and to strains effects originating from the Mn dopant, denoted as $\Delta H_{def}$.

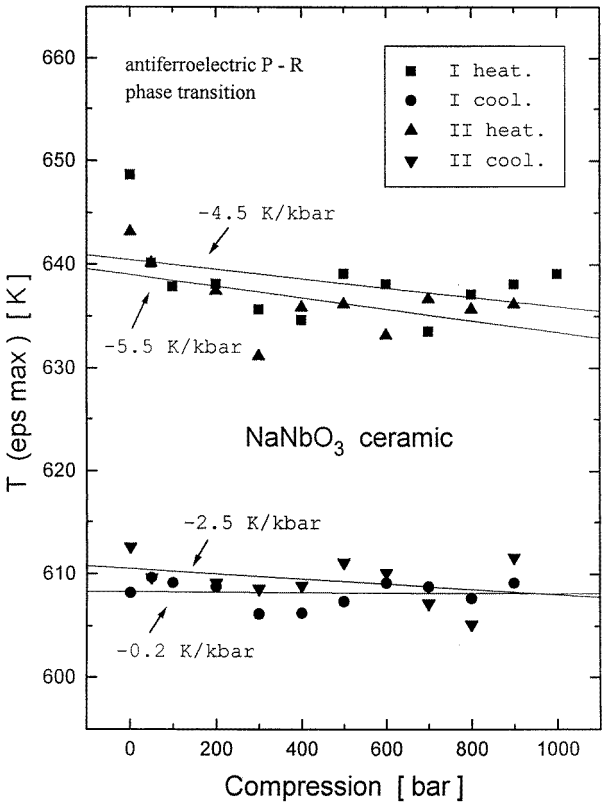


**Figure 6.** Antiferroelectric P–R phase transition temperature–axial compression dependency for ceramic $NaNbO_3$ received from maxima in dielectric permittivity $\varepsilon(T, p)$ curves. Linear fits are shown: $-4.5$ K kbar$^{-1}$ (first heating), $-5.5$ K kbar$^{-1}$ (second heating), $-0.2$ K kbar$^{-1}$ (first cooling), $-2.5$ K kbar$^{-1}$ (second cooling).

In the case of the P–R phase transition of $NaNbO_3$ the latent heat is 340 ($\pm$15%) J mol$^{-1}$; polarization $P_s = 0$ leads to $\Delta H_{el.ord} = 0$. It is impossible to determine precisely the elastic enthalpy component $\Delta H_{elast}$ due to the stiffness constant having not been measured. However, the specific strain tensor components have been calculated [10, 41] based on the Roitburd theory applied to the sodium niobate phase transitions. In the case of the concerned orthorhombic P–R phase transition, the reported values are $e_a = \Delta a/a_o = -0.001\,1722$, $e_b = \Delta b/b_o = 0.001\,4051$, $e_c = 0$, $t = \tan((\delta - 90^\circ)/2) = 0.0017$ (*a, b, c* refer to the lattice parameters, $t$ to the angle of monoclinic deformation of pseudocubic subcell). The values of strain tensor components listed here for $NaNbO_3$ are lower but comparable to those of $BaTiO_3$. Instead of adequate calculations, it is justifiable that the elastic component in enthalpy change could be taken as $\Delta H_{elast} \cong -10^2$ J mol$^{-1}$ (common order for perovskites). Under such an assumption, one can obtain for the P–R phase transformation in sodium niobate

$$\sum_i \Delta H_i = L + \Delta H_{elast} + \Delta H_{def} \cong 340 - 100 + \Delta H_{def}. \tag{6}$$

This sum is expected to be equal to the enthalpy obtained by DTA. Since $Q_{DTA} = 220$–360 J mol$^{-1}$ depends on the Mn dopant concentration, one can estimate the defect subsystem

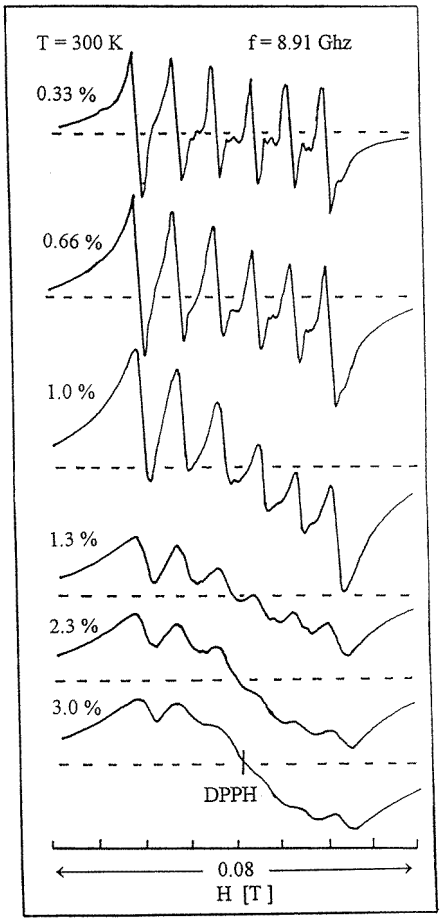


**Figure 7.** EPR spectra of $NaNbO_3$:$x$Mn ($x = 0.33, 0.66, \ldots,$ 3mol%) recorded in X-band at room temperature. The evolution of the h.f.s. spectrum originating from $Mn^{2+}$ paramagnetic centres as a function of Mn dopant concentration is visible.

contribution $\Delta H_{def}$ as varying in the 0–100 J mol$^{-1}$ range with Mn concentration increase.

The analysis conducted above shows that the dopant subsystem introduces internal strains and affects the P–R phase transition in the investigated sodium niobate samples. The appearance of disorder and internal strains caused by the Mn dopant has been confirmed with the EPR test. The discrepancy between ionic radii of the sodium niobate host and the dopant support this conclusion. The charges of heterovalent $Mn^{2+}_{Na}$ ions built into the sodium sublattice of $Na^+Nb^{5+}O^{2-}_3$:Mn are mostly compensated by oxygen vacancies forming $Mn^{2+}$–$V'_O$ centres [26]. In this case the radius of $Mn^{2+}$ ions (0.083 nm) is smaller than the radius of $Na^+$ ions (0.102 nm). Charge compensation by niobium valence change in $Mn^{2+}_{Na}$–$Nb^{4+}$ centres is also possible and the $Nb^{4+}$ radius (0.068 nm) is larger than the $Nb^{5+}$ radius (0.064 nm). Even if some of the manganese ions replace niobium ions as $Mn^{4+}_{Nb}$, then the $Mn^{4+}$ ionic radius (0.053 nm) is smaller than the $Nb^{5+}$ radius. Such a relation between ionic radii in the induced centres should cause shrinking of the doped sodium niobate lattice.

As found for $NaNbO_3$, the external compression shifts the P–R phase transition by $-5+-6$ K kbar$^{-1}$ (a discrepancy observed on cooling would be caused by irreversible effects, possible due to interaction of defects). This may be compared to the shift caused by internal strains due to the doping. It is seen from the phase diagram (figure 2) that the temperature of the P–R phase transition is lowered by approximately 50 °C with the Mn concentration approaching 1 mol%. Thus one may presume that the strain effects caused by the Mn dopant are equivalent to external pressure of the order of 10 kilobars.

The indirect observation of the phase transition kinetics is possible by use of the characteristics of dielectric permittivity. The correspondence between the steplike $\varepsilon(T)$ curve and optically observed pinning of interphase boundary has been stated for another phase transition (P–N) in $NaNbO_3$:Mn [42]. Thereby, one can deduce that recorded mean values of $\varepsilon(T)$, in accord with (1), reflect the mixed state of the sample within the phase transition range.

The influence of the strains on the kinetics of the antiferroelectric and ferroelastic phase transition is visible clearly in the steplike dielectric permittivity curve recorded for $NaNbO_3$ crystals (see figure 5). It should be pointed out that a few hundreds of bars (more than 100 bar) is sufficient to suppress a one-step jump in $\varepsilon(T, p)$ behaviour. Such effect manifests the jerky motion of the phase front stopped by the existing local strains around defects. A smeared and almost smooth $\varepsilon(T)$ curve is recorded at compression approaching 1000 bars. This means the phase transition occurs step by step in small volume fragments of the compressed crystal sample.

A similar effect has also been observed on sodium niobate crystals slightly doped with manganese ($N_{Mn} \approx 0.1$ mol% [25]) where the steplike $\varepsilon(T)$ curves are recorded even for non-compressed samples. When pressure is applied then this effect becomes more remarkable, i.e. more steps in a wider temperature range appear [42, 43]. Pressure induced smearing of the $\varepsilon(T, p)$ characteristics, visible for the investigated ceramics, reinforces such an explanation. The internal strains may be considered as the factor causing the smooth smeared shape of the $\varepsilon(T)$ characteristic although transformation between P and R phases in sodium niobate persists as the first-order transition.

The time-dependent Ginzburg–Landau equation describes the interphase motion as a moving kink. Its basic solution gives the kink which propagates with stable velocity which is scaled by such factors as stress or defect concentration [5–8]. This solution describes adequately the kinetic of the P–R phase transition in the non-compressed crystal samples (see figure 3(a)). However, a more complicated situation is detected in compressed or Mn doped sodium niobate. When strains in these samples are increased then the jerky movement of the interphase front is enhanced, reflecting different states of motion of the interphase boundary.

From the literature reports [9, 10] it is known that such a jerky movement is the result of switching between slow and fast motion of the interface boundary. This unstable kinetic may be explained within a generalization of the kink model where the switching between slow and fast motion is ascribed to polarization and stress decoupling [44]. Circumstances for such a switching could be temperature or strain inhomogeneity. It should be mentioned that the subsystem of the Mn dopant in $NaNbO_3$ carries in an additional amount of enthalpy $\Delta H_{def}$ detected by DTA. However, from the point of view of the kink motion model developed for perovskites, the release of energy near the moving phase front ought to be meaningless due to high heat conduction in these materials [7]. Due to such restrictions, the effective temperature should be homogeneous within the sample. On the other hand, the performed compression and dopant ions create local heterogeneous strains which produce barriers to the motion of interphase front connected with the dislocation boundary. Under

the circumstances of the performed temperature run, it is equivalent to the appearance of overheated or overcooled areas near the interacting obstacles. Therefore one can say that the inhomogeneous stress fields cause a spatial variation of the transition temperatures, adequate for the fracture volumes, within the samples of Mn doped $NaNbO_3$. Such stress fields lead to the step-by-step occurrence of the investigated phase transition within an interval of temperatures.

The phenomena discussed above involve strains and defects as main factors modifying the investigated antiferroelectric, ferroelastic, first-order structural displacive phase transition (called P–R) in sodium niobate.

The similarity should be noted between the concepts of the displacive and martensitic transformations because of the characteristic coordinated atomic movement through the interface. Moreover, since a distortion of the lattice is a general feature of martensitic transformations, many of them fulfil the properties of ferroelastic phase transitions [3, 10, 45–48]. One can find a few models which describe such phase transitions as a function of the strains or defect concentration.

(i) The influence of defects on first-order structural phase transitions has been studied using the mean-field thermodynamic potential [49]. It is shown that the defect contribution, proportional to their concentration, causes smearing of the first-order phase transition: decreasing of jumps of various thermodynamic quantities at the phase transition are expected. The results obtained within this phenomenological approach may qualitatively describe the phase transition in sodium niobate although the model, considering elastic deformations in an isotropic medium and an order parameter which has symmetry properties different from those of the components of strain tensor, idealizes the real crystals.

(ii) Another model is developed within the Landau theory of ferroelastic phase transitions [39]. An interaction of a phase front and a defect has been proposed to describe the direct observations of the phase front stopping in sodium niobate and lead hafnate crystals. It is shown that the phase front can be locked by the inhomogeneous elastic field raised by a pre-existing twin boundary. The case of joint motion of the twin boundary and phase front may be realized if an applied pressure overcomes a maximum value $\sigma_{max}$ of the pressure due to the interaction of the twin boundary with the locking defect. The value of such a pressure $\sigma_{max}$ is estimated as 0.01–0.1 bar [39].

However, this model does not deal with the case of stronger external pressure which may affect or create locking centres.

(iii) Although there are still controversies about the classification of whether a transformation is a martensitic one, this transformation is usually described as being: (a) diffusionless, (b) displacive, (c) first order, (d) mediated by a habit plane resulted from invariant plane strain condition and (e) dominated by the strain energy involving lattice distortion of 'shear-like' type [3, 36, 40, 47, 50].

The discussion about the features of martensitic transformation in sodium niobate is possible after the examination of the properties (a)–(e). The transition between P and R phases, connected to Nb ion displacement within oxygen octahedra, occurs with the monoclinic distortion of the pseudoperovskite cell. Indeed, the properties (a)–(c) are fulfilled as determined by x-ray [12, 13, 14, 23], optic, dielectric and specific heat [24, 43] investigation.

The study [41] of orientation of phase boundaries allow us to determine the components of the specific strain tensor (their values are listed in the text, above (6)). In the case of the P–R phase transition, apart from the dilatation of the pseudoperovskite unit cell, also angular strain (shear) takes place. It occurs that in the framework of Roitburd theory [10, 11, 41]

the P–R phase transition belongs to the class in which the specific strain is a strain with invariant plane. The presented crystallogeometric relations of interphase boundaries indicate that the P–R transition in sodium niobate exhibits features characteristic of martensitic transformation [41].

The importance of strain energy at the phase transition (property e) is stated in this work as well in the literature. The shear strain is involved at the transition between the P and R phases [10, 41]. It is shown that the transition temperature and the movement of the interface is influenced by external pressure [16, 23, 43]. The interaction of this transformation with structural defects like impurities or dislocations [9, 10, 27, 39, 42] remains also in agreement with martensitic transformation dependencies [3, 40, 47, 48, 50].

One can notice that these properties of the P–R phase transition in sodium niobate are sufficiently convergent to the features of martensitic transformation.

The range of the martensitic transformation, starting from temperature $T_S$ and completed at the martensite finish temperature $T_M$ can be estimated from variety of derivatives of dielectric permittivity $\Delta\varepsilon/\Delta T$ shown in the insets in figures 3 and 5. For the non-stressed sample the transformation occurs in one jump (figure 3(a)) and then $T_S$ equals $T_M$ practically. In the case of stressed samples, one can easily distinguish the starting $T_S$ and finish $T_M$ temperatures (see insets in figure 3(b), (c)) as the temperatures limiting an interval within which $\Delta\varepsilon/\Delta T$ take markedly high values. It may be estimated that the compression applied within the range of 1 kbar causes the $T_S$–$T_M$ range increase up to a few degrees for the $NaNbO_3$ crystal (see figure 3). This effect may be regarded as even more distinct for the ceramic samples (figure 5). Therefore these results lead to the conclusion that local strains, originating from compression or Mn dopant, induce athermal martensitic behaviour of the transformation between P and R phases in sodium niobate.

## 5. Conclusions

(1) Manganese dopant induces disorder and strains in the $NaNbO_3$ samples, detected by the EPR test.

(2) The axial compression causes the lowering of the P–R phase transition temperature. The values of the shift are $\partial T_{P-R}/\partial p = -5 \pm 1$ K kbar$^{-1}$ for ceramic samples and $-6 \pm 1$ K kbar$^{-1}$ for single crystals of $NaNbO_3$. The strain effects caused by 1 mol% of the Mn dopant is equivalent to external pressure of the order 10 kbar.

(3) It has been found that local strains, caused by Mn dopant or external compression, influence the kinetic of the phase front in sodium niobate. The steplike characteristics of dielectric permittivity in the range of first-order phase transition are observed due to the phase front stopped on local strains. The athermal martensitic behaviour of the ferroelastic and antiferroelectric P–R phase transformation in sodium niobate is enhanced by applied compression.

## Acknowledgments

The author thanks Professor Jan Hańderek for helpful discussion and Professor Jan Dec for supplying $NaNbO_3$ single crystals and for helpful discussion.

## References

[1] Salje E K H 1990 *Phase Transitions in Ferroelastic and Co-elastic Crystals* ed E K H Salje (Cambridge: Cambridge University Press)

[2] Pietrass B 1975 *Phys. Status Solidi* b **68** 553
[3] Cao W, Krumhansl J A and Gooding R J 1990 *Phys. Rev.* B **41** 11 319
[4] Fradkin M A 1994 *Phys. Rev.* **50** 16 326
[5] Gordon A and Dorfman S 1995 *Phys. Rev.* B **51** 9306
[6] Gordon A, Dorfman S and Wyder P 1995 *J. Phys.: Condens. Matter* **7** 9905
[7] Gordon A, Dorfman S and Fuks D 1996 *J. Phys.: Condens. Matter* **8** L385
[8] Gordon A 1991 *Phys. Lett.* **154A** 79
[9] Dec J 1989 *Ferroelectrics* **89** 193
[10] Dec J 1993 *Phase Transitions* **45** 35
[11] Roitburd A L and Kurdjumov G V 1979 *Mater. Sci. Eng.* **39** 141
[12] Glazer A M and Megaw H D 1973 *Acta Crystallogr.* A **29** 489
[13] Megaw H D 1968 *Acta Crystallogr.* A **24** 589
[14] Lefkowitz I, Łukaszewicz K and Megaw H D 1966 *Acta Crystallogr.* **20** 670
[15] Zhelnova O A, Fesenko O E and Smotrakov V G 1986 *Sov. Phys.–Solid State* **28** 144
[16] Pisarski M 1980 *Acta Phys. Pol.* A **57** 693
[17] Gejfman I N, Glinchuk M D, Bykov I P, Rozkho V S and Krulikovskij 1976 *Fiz. Tverd. Tela* **18** 2642
[18] Ahtee M and Glazer A M 1976 *Acta Crystallogr.* A **32** 434
[19] Rajevskii I P, Smotrakov V G, Lisitsyna S O, Zajtcev S M and Selin S V 1985 *Neorg. Mater.* **21** 846
[20] Iwasaki H and Ikeda T 1963 *J. Phys. Soc. Japan* **18** 157
[21] Ellis B, Doumerc J-P, Pouchard M and Hagenmuller P 1984 *Mater. Res. Bull.* **19** 1237
[22] Molak A 1988 *Ferroelectrics* **80** 27
[23] Molak A, Pawełczyk M and Kwapuliński J 1994 *J. Phys.: Condens. Matter* **6** 6833
[24] Cross L E and Nicholson B J 1955 *Phil. Mag.* **46** 453
[25] Molak A and Jelonek M 1985 *J. Phys. Chem. Solids* **46** 21
[26] Molak A 1987 *Solid State Commun.* **62** 413
[27] Dec J 1983 *Cryst. Res. Technol.* **18** 195
[28] Molak A and Pichet J 1984 *Acta Phys. Pol.* A **66** 251
[29] Misra S K 1994 *Physica* B **203** 193
[30] Nambu S and Sagala D A 1994 *Phys. Rev.* **50** 5838
[31] Bratkovsky A M, Marais S C, Heine Volker and Salje E K H 1994 *J. Phys.: Condens. Matter* **6** 3679
[32] Salje E, Bismayer U, Wruck B and Hensler J 1991 *Phase Transitions* **35** 61
[33] Levaniuk A P and Sigov A S 1988 *Defects and Structural Phase Transitions* (New York: Academic)
[34] Eyraud L 1967 *Dielectriques Solides Anisotropes et Ferroelectricite* (Paris: Gauthier–Villars)
[35] Pertsev N A and Arlt G 1991 *Ferroelectrics* **123** 27
[36] Warlimont H and Delaey 1974 *Martensitic Transformations in Copper–Silver and Gold-Based Alloys (Progress in Material Science, 18)* ed B C Chalmers, J W Christian and T B Massalski (Oxford: Pergamon) pp 91–106
[37] Hull D and Bacon D J 1984 *Introduction to Dislocations* (Oxford: Pergamon)
[38] Gridnev S A, Darinskii B M and Prasolov B N 1983 *Ferroelectrics* **48** 169
[39] Balyunis L E, Bulbich A A and Zhelnova O A 1993 *J. Phys.: Condens. Matter* **5** 4149
[40] Vul D A and Harmon B N 1993 *Phys. Rev.* B **48** 6880
[41] Dec J and Kwapuliński 1989 *Phase Transitions* **18** 1
[42] Molak A, Onodera A and Yamashita H 1992 *Japan. J. Appl. Phys.* **31** 3221
[43] Molak A, Onodera A and Pawełczyk M 1995 *Ferroelectrics* **172** 295
[44] Tuszyński and Sept D 1994 *J. Phys.: Condens. Matter* **6** 3583
[45] Mnyukh Yu V, Panfilova N A, Petropavlov N N and Uchvatova N S 1975 *J. Phys. Chem. Solids* **36** 127
[46] Pouget J 1991 *Phase Transitions* **34** 105
[47] Guenin G 1989 *Phase Transitions* **14** 165
[48] Kartha S, Krumhansl J A, Sethna J P and Wickham L K 1995 *Phys. Rev.* B **52** 803
[49] Levanyuk A P, Minyukov S A and Vallade M 1997 *J. Phys.: Condens. Matter* **9** 5313
[50] Lovey F C and Torra V 1995 *J. Physique Coll.* IV **5** C2 235